

AN EXPERIMENTAL STUDY OF STIFFENED OPEN-HOLE COMPOSITE PANEL WITH BVID UNDER UNIAXIAL COMPRESSION

Jianzhuo Sun, Qun Zhao, Peng Shi, Hainan Yang and Chuanjun Liu

Beijing Key Laboratory of Civil Aircraft Structures and Composite Materials, Beijing Aeronautical Science & Technology Research Institute of COMAC, Future Science and Technology Park, sunjianzhuo@comac.cc

Keywords: Composites, BVID, Open-hole Panel, Stiffened Panel, Axial Compression Test

ABSTRACT

An experimental study is conducted to validate a finite element method for a stiffened open-hole composite panel under uniaxial compression. An axial released jig is designed and built to provide the transverse support on the specimen. Two BVIDs (Barely Visible Impact Damages) are introduced on the specimens before loading. Non-destructive inspection equipment is used to investigate the locations, dimensions, and extensions of the damages. Acoustic emission inspection equipment is employed and set on the specimens to detect the position and timing of damage occurring. The strain deviations between test and analysis results at the critical locations are less than 8% at 100% DLL load.

1. INTRODUCTION

Carbon fiber composites are employed more often in commercial and military transport aircraft in the past several years, due to the valuable in-plane properties. However, their wider spread use is limited by the relative unsatisfactory of the out-of plane properties, such as low resistance to impact. A low velocity impact with certain energy can cause delamination, matrix cracking, and other issues, which are barely visible, to the composite. More important, such damage may reduce the compressive strength significantly [1-3].

Due to the high cost of manufacturing and testing structural specimens, a large amount of literature about impact damage effect on composite is available for coupon level tests [1-3]. However, some literature is given that the introduced damage is less severity on structures than the damage on coupons at the same impact energy [4]. It is suspected that part of the energy is dissipated through the structure. To fully understand the low velocity impact effect in real situation, structural specimens have to be tested. Recently, impact damage effect on compressive properties of stiffened panel, which is widely used in typical aircraft structure such as a fuselage shell or a wing surface, is investigated in quite a few works [4-8].

In reality, for many practical concerns, such as hydraulic lines, damage inspection and windows, open cut-outs are required to be designed on the stiffened panel. At the meanwhile, cut-outs introduce stress concentration in structures, which can initiate damage and early failures. In recent years, some works have been done to study the mechanical behaviour and predict the failure strength of stiffened composite panels with cut-outs [9-11]. However, not much work has been done to study the impact damage effect on stiffened panel with cut-outs.

In this study, efforts are made to study the compressive response of stiffened panel with coupling effect of cut-outs and impact damage.

2. EXPERIMENTAL

2.1 Specimen Design and Manufacture

To fulfil the airworthiness requirements of accessibility and inspect ability, the commercial aircraft is designed with man-hole on the lower panel of wings. The specimen, made up is a skin, two stringers and two cut-outs are simplified from typical lower panel structures around manhole.

Since lower panel of wing is primary structure, the specimen is manufacture from T800 level prepreg. The skin is 9 mm thick. The stringers are 440 mm apart each other, and have a T-section.

Each stringer was assembled from four uncured laminates, forming a tapered base, two L-sections, back to back, and an inserted laminate. After that the assembled stringers are cured with a dry skin.

To increase the strength of the clamped section, the flanges of stringers are widened and two reinforced pads are added on both ends of specimen. To transform the compressed load, two aluminium powders reinforced resin holders are fixed on the ends of specimen, which is shown in Figure 1.

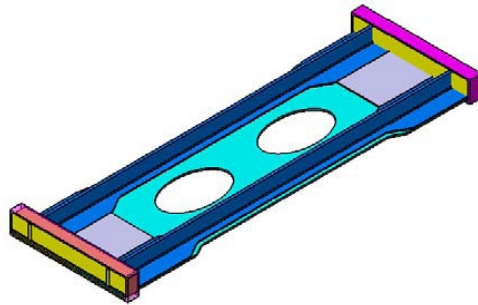


Figure 1: Schematic of specimen

2.2 loading Device and Test Jigs

In this study, a MTS is employed as loading device, of which capacity is 200T. A flat platform is fixed on the actuator of the MTS to provide the displacement of the specimen. Another platform is assembled on a universal joint, which is set on the ground, to guarantee that the load applied on the specimen is uniaxial.

In an aircraft, ribs form a skeletal shape for the wing. At the meanwhile, ribs support the upper and lower panel and constrain the out-of plane displacement of the skin. To decrease the assembled difficulty of the specimen, wing ribs are replaced by an axial released jig. To simulate the functional of ribs, three pieces of jig are placed 580 mm apart from each other on the specimen. The schematic of the test equipment is shown in Figure 2.

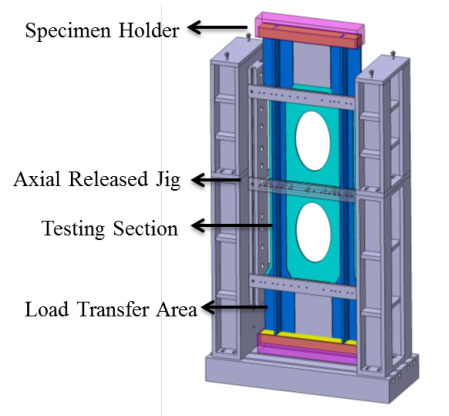


Figure 2: Schematic of loading condition

2.3 Impact Introduction

Before loading, to introduce the BVIDs on the specimen, the top edge of stringer and the short-axis edge of man-hole are impacted by drop-weight tower. The locations are shown in Figure 3. The instrument has a 16 mm diameter hemispherical tup. For web edge impact, the energy is required as 10 J. For the impact near man-hole, the energy is required as 35 J. The aforementioned jigs are fixed on the rib positions to simulate the supports by ribs in the aircraft.

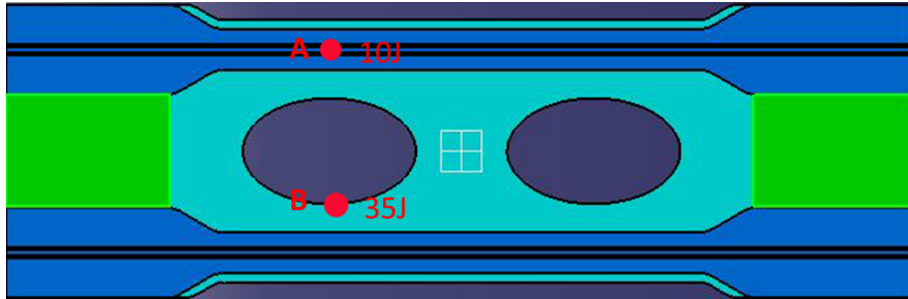


Figure 3: Impact position and impact energy



Figure 4: Impact device

2.4 Strain Gauges

To investigate the maximum strain and strain distribution of the specimen, strain gauges are bonded to the panels. All the strain gauges are placed back to back, to monitor the buckling of the specimen. The locations and numbers of strain gauges are shown in Figure 5. The numbers in the brackets are the numbers of strain gauges on the backside of the skin.

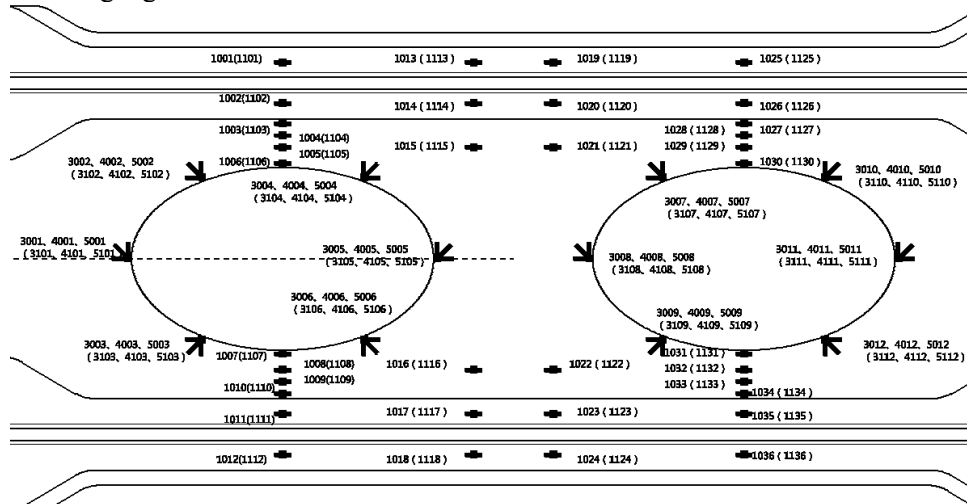


Figure 5: Locations and numbers of strain gauges

2.5 Acoustic emission Device

When determining the failure mode of the specimen, locating the first failure position of the structure is imperative. Thus, acoustic emission device is utilized to record the barely audible acoustic wave from structural break during the test. Totally, 16 sensors are attached at different locations on the specimen and capture the sound wave, as shown in Figure 6. A PAC Express 8 device, as shown in Figure 7, is used in this study.

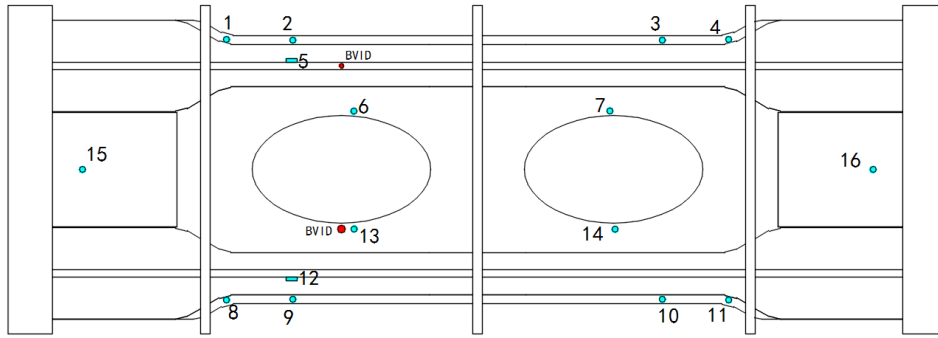


Figure 6: Locations and numbers of acoustic sensor



Figure 7: PAC Express 8 system

2.6 Test procedure

Firstly, the specimen is loaded up to 60% DLL by the increment of 5% DLL, and then unloaded. This test will keep repeating until the differences of strain signals from symmetric locations are less than 5%. Secondly, the specimen is loaded up to 110% DLL by the increment of 5% DLL, the load would be hold for 30 seconds. After unload, the non-destructive inspection is conducted to inspect the damage extension of the specimen. And then the specimen is loaded up to 165% DLL, the load would be hold for 3 seconds. Finally, the load would keep going up by 1% DLL per step until the specimen is compressed to failure.

3. FINITE ELEMENT MODEL

The Finite element model is created in Hypermesh. The skin, stringers and reinforced panel are modelled by shell elements. The holders are modelled by solid element. It is important to note that the interfaces between skin and stringers, skin and reinforced panels are modelled by RBE3 elements, which are constrained the relative displacement between each parts. The load point is set on the stiffness centre of loading surface, to eliminate the extra bending effect. On the other end, the edge is fixed with six freedoms. The FE model of specimen is shown in Figure 8.

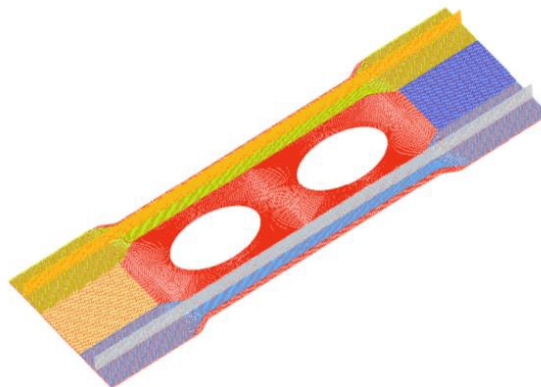


Figure 8 Finite element model of specimen

The buckling load of the specimen is predicted as 340% DLL, by using the eigenvalue method. The displacement contour of the specimen at the first buckling mode is plotted in Figure 9. The strain contour of X-direction is obtained by using the aforementioned FE model at 150% DLL, which is shown in Figure 10.

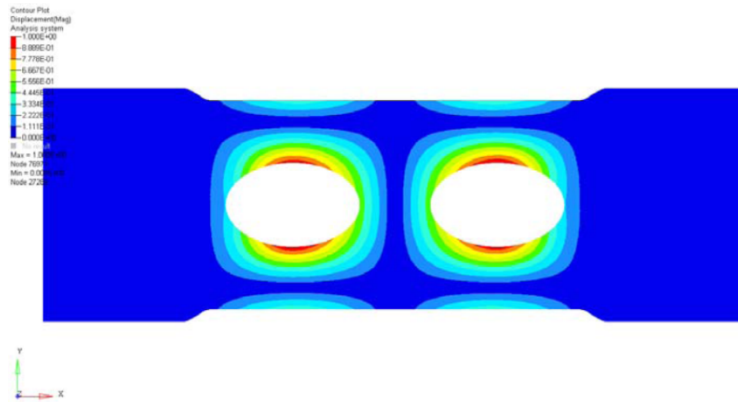


Figure 9: Contour of displacement

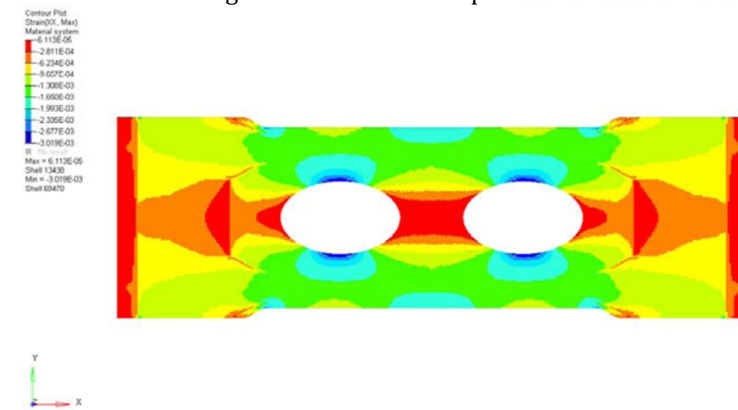


Figure 10 Contour of Strain

4. RESULT AND DISCUSSION

After the specimen was impacted by the drop weight tower, the area around the impact position was inspected by the C-scanned device, and the depth of the dent was measured by a calliper. The inspection results are shown in Table 1. The delaminated area of the stringer around A area is shown in Figure 11. For the B position, no delamination was found.

Table 1 Inspection Results

	Impact Energy	Depth of Dent	Delamination area
Position A	10.07 J	0.12 mm	508 mm ²
Position B	35.23 J	0.08 mm	0



Figure 11 Delamination area of A position

During 110% DLL loading test, the strain gauge signals show good agreements with the FE results, the differences between each other are less than 7%. However, the acoustic emission sensors around the manhole impact position (sensor #9, #12, #13) start to receive the irregular signal from 70% DLL, which is shown in Figure 12. The C-scanned result shows that there is no delamination at impact A position, but the stringer and skin got deboned, as shows in the red section in Figure 13. Since the signal of acoustic sensor is relatively low and there is no de-bounding sound heard by human ears. It is highly suspected that the impact near the manhole results in the detachment of the stringer and skin, though the de-bonded area wasn't scanned by the NDI device before test.

Signal Strength (pVs) VS Time (s)

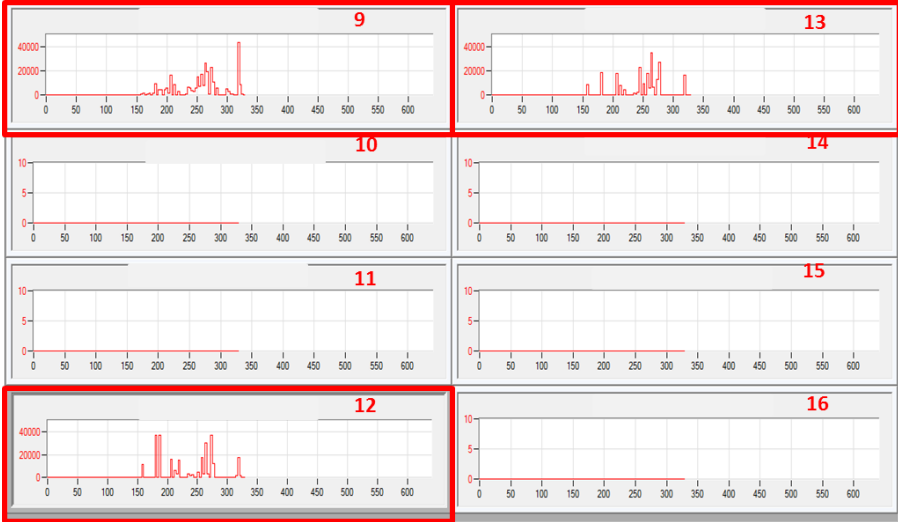


Figure 12 Acoustic sensor signals (9-16) of 110% DLL



Figure 13 Detachment area of stringer

In the specimen failure test, the acoustic sensors around the manhole impact position (sensor #9, #12, #13) start to receive the irregular signal from 70% DLL as well, which may indicate that the initial detachment begin to grow gradually after 70%DLL. The magnitude of the signal increase dramatically after the specimen loaded to 200% DLL, which shows that the detachment expands much faster than the expansion at lower load. The signals from the sensors, which are located on the opposite side of the manhole to the impact position (sensor #1, #2, #5), has no change until the load goes up to 220% DLL. After that, the sensor receive a pulse signal, but there is no significant noise heard by human ears, which may inform that the stringer and skin get deboned rather than material failure. After a few seconds, with a huge noise, the signals go up to a very high level, which is shown in Figure 14&15. The stiffened panel get crashed at 229% DLL.

Signal Strength (pVs) VS Time (s)

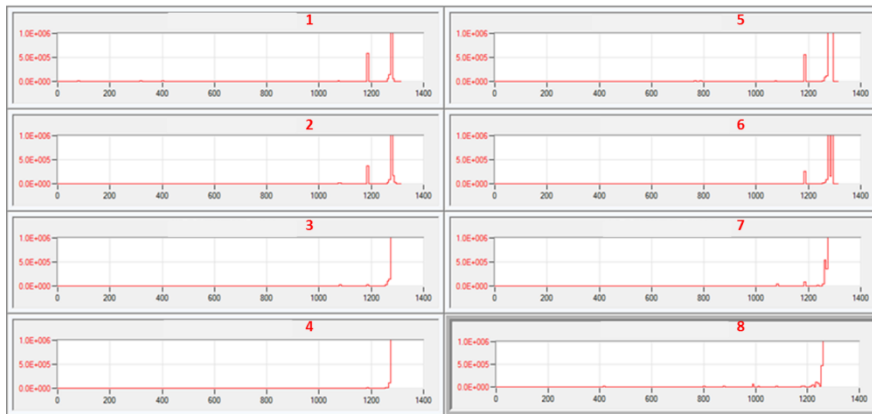


Figure 14 Acoustic sensor signals (1-8)

Signal Strength (pVs) VS Time (s)

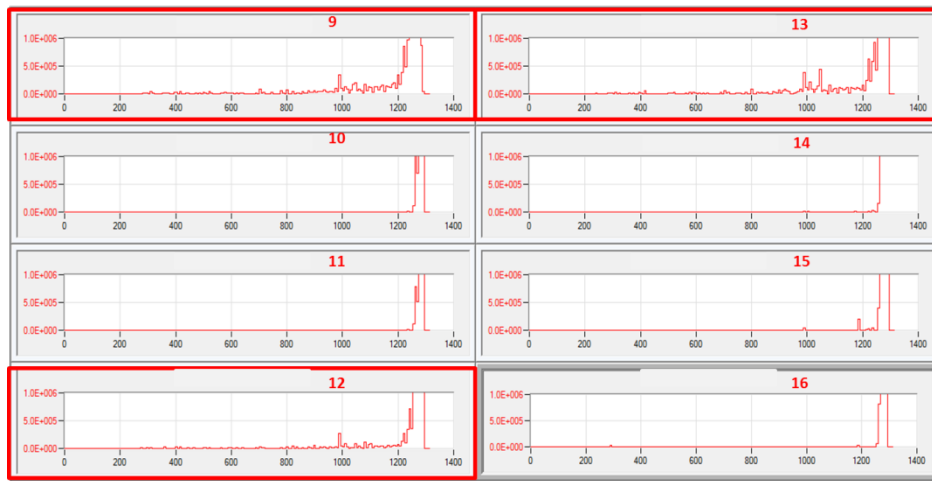


Figure 15 Acoustic sensor signals (9-16)

For the strain measurements, when the load goes higher than approximate 130% DLL, the back to back strain gauge signals (1007/1107, 1008/1108, 1009/1109, 1010/1110) around the impacted position become diverged, which is near the man-hole. The signals of 1007 and 1107, where located at B impact position as show in Figure 16, are compared with the FE results and shown in Figure 16. The divergence increase dramatically after the load goes higher than 200%, which is at the same time that the acoustic signals enlarge significantly. Besides, the signal of 1012 located on the stringer keeps being linear, but the signal of 1112 located on the backside of the skin goes down, which is shown in Figure 17. In summary, it is inferred that the stringer and the skin got massively de-bonded after the load reached 200% DLL, and the skin became highly buckled until the material failed. The crashed specimen is shown in Figure 18. The skin is broken, and detached with the stringer. The failure mode is the same as the inference from the acoustic signals and strain gauge signals.

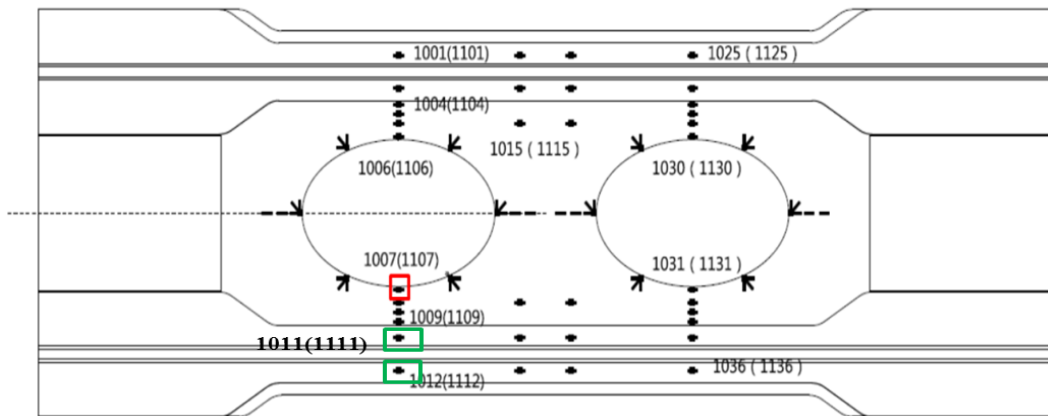


Figure 16: Strain Gauge Location

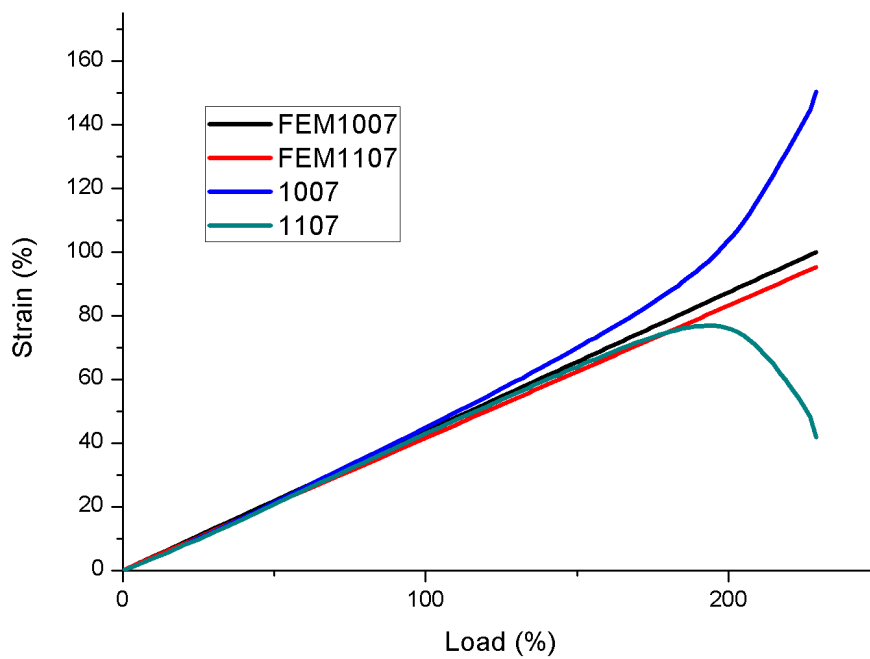


Figure 17 Strain Comparison

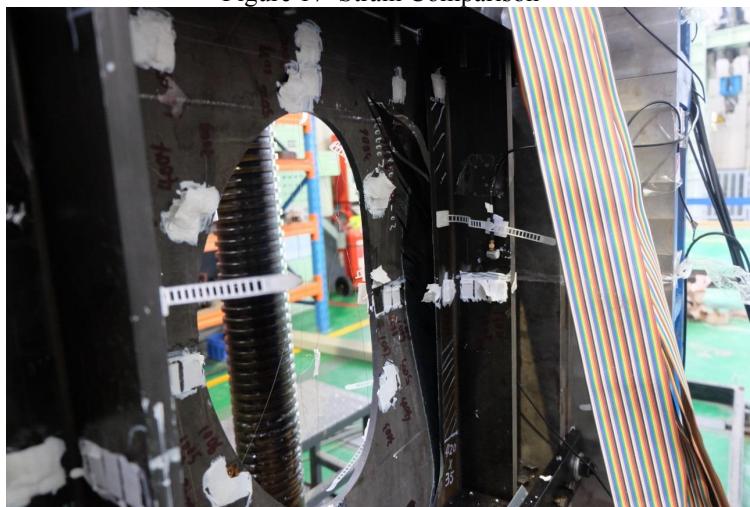


Figure 18: Crashed Specimen

From the results of this study it can be suggested that the incident impact energy could cause damages not only at the impact position, but also the area around it, especially the impact position is at

the edge of structures. The stress wave would go back from the free edge, and propagate to the other structures. If the interfaced bonding is not strong enough, it may cause unexpected de-bonds. Although the detachment is extremely fatal, it is barely visible. To avoid the detachment, fasteners are suggested to install at such positions.

5. CONCLUSION

In this study, a stiffened open-hole composite panel was designed and manufactured. Two impacts were introduced on stringer and skin. The specimen was compressed under uniaxial load. Acoustic emission and strain gauges were used to monitor the test process. The FE model was validated at linear region. The specimen got failure because of the detachment between skin and stringer. It is suggested that fasteners should be installed at the position, which is near the short-axis of the manhole, on the stringers. Impact energy effect on the detachment need to be investigated in the future.

REFERENCE

1. D. Hull and B. Y. Shi: *Compos. Struct.*, 1993, 23, 99–120.
2. W. Cantwell and J. Morton: *Compos. Struct.*, 1990, 14, 303–317.
3. J. Williams, M. Rhodes, J. Starnes, and W. Stroud: *Proc. 8th Conf. 'Fibrous composites in structural design'*, 1989, Department of Defence–National Aeronautics and Space Administration–Federal Aviation Authority, Part 1, pp. 259–290.
4. Greenhalgh, E.S., Bishop, S., Bray, D., Hughes, D., Lahiff, S., Millson, B. (1996) “Characterisation of impact damage in skin-stringer composite structures”, *Composites Structures*, 36(3-4), 187-207.
5. Greenhalgh, E., Singh, S., Hughes, D., Roberts, D. (1999) “Impact damage resistance and tolerance of stringer stiffened composite structures”, *Plastics, Rubber and Composites*, 28(5), 228-251.
6. Greenhalgh, E., Hiley, M. (2003) “The assessment of novel materials and processes for the impact tolerant design of stiffened composite aerospace structures”, *Composites Part A: Applied Science and Manufacturing*, 34, 151-161.
7. Jegley, D.C. (1992) Effect of low-speed impact damage and damage location on behavior of composite panels, NASA Technical Paper 3196.
8. Jegley, D.C. (1998) Behavior of compression-loaded composite panels with stringer terminations and impact damage, AIAA Paper 98-1785-CP.
9. Nemeth, M.P. (1996) Buckling and post buckling behavior of laminated composite plates with a cut-out, NASA Technical Paper 3587.
10. Guz IA, Soutis C, Zhuk Y. (2012) Compressive response of composite stiffened panels with open holes. In: “Encyclopedia of Composites”. Vol.1-5 (Eds: L. Nicolais, A. Borzacchiello, S.M. Lee). Vol.1, John Wiley & Sons, pp.585-594.
11. Buckling and Postbuckling Studies on Stiffened Composite Panels with Circular Cutouts